Post-processing method for predicting NO formation in one-dimensional and two-dimensional premixed methane-air flames

Post-Processing Method for Predicting *NO* Formation in One- and Two-Dimensional Premixed Methane-Air Flames

R. L. G. M. EGGELS and L. P. H. DE GOEY*

Eindhoven University of Technology, Faculty of Mechanical Engineering (WH3.135), Eindhoven, The Netherlands

A post-processing method to predict *NO* formation in one- and two-dimensional flames is developed. A flame calculation with a reduced number of species and reactions is performed first. The remaining species are computed in a post-processing step. The computational effort is reduced further by introducing steady-state assumptions for intermediates.

The results of the post-processing method applied to adiabatic flat flames agree well with complex calculations. Computations of burner-stabilized flames are compared with results of measurements on a ceramic foam surface burner, and the agreement is satisfactory. The post-processor method makes it possible to perform two-dimensional detailed *NO* computations within a reasonable computing time. As an example, results for a two-dimensional slot burner in a confined environment with cold walls are presented.

1. INTRODUCTION

To reduce environmental pollution, regulations concerning *NO* emissions have become more stringent recently. A reduction in the emission of *NO* requires increasing knowledge of *NO* formation in combustion processes. From a chemical point of view, the formation of *NO* in methane-air flames is reasonably well understood [1] and has led to the development of detailed reaction mechanisms, involving a large number of species and reactions. One such example is the scheme of Miller and Bowman [2], which consists of 51 species and over 200 reactions. There are, however, relatively large uncertainties in the reaction rate data. If more recently published reaction rate data are used [3], significant deviations in *NO* concentrations at a distance of one centimeter above a flat burner are observed [4]. Apart from such uncertainty, the use of such complex reaction schemes leads to extravagant computational effort for realistic combustion processes. Reduced models to predict *NO* formation are therefore required. In this paper, we present a post-processing method for computing *NO* concentration in one- and two-dimensional laminar methane-air flames. Basically, we follow the approach of Glarborg et al. [3], who presented a post-processing method for a perfectly stirred reactor, which has been extended recently to one-dimensional flames. First results [4] showed that various reaction mechanisms lead to quit large differences in *NO* mole fractions. Here it is shown that this is caused by differences in burning velocity and variations in equilibrium composition. These effects can be eliminated by considering adiabatic flames and by assuming that all reactions are reversible. Furthermore, computations are compared with measurements, and the method is extended to model *NO* formation in two-dimensional flames.

We were able to investigate the magnitude of the contribution of the thermal *NO* mechanism to the total *NO* formation. The difference between the two is referred to as prompt *NO*. Hence *NO* concentrations are computed using the detailed reaction mechanism, as well as the Zeldovich reactions only.

The post-processing method is presented in Section 2, followed by the method of discretization, in Section 3. The results of the post-processing method for one-dimensional flames using different reaction schemes are compared with complex computations and measurements on a ceramic foam burner in Section 4. Finally, the results of two-dimensional computations, of a single-slot burner in a confined environment with cooled walls, are presented in Section 5.

2. POST-PROCESSING METHOD

The post-processing method is based on the assumption that the species involved in *NO* chemistry have very low mass fractions and a

* Corresponding author.

COMBUSTION AND FLAME 107: 65–71 (1996)

Published by Elsevier Science Inc.

0010-2180/96/$15.00
PII S0010-2180(96)00017-X

minor influence on the major combustion species. The reaction scheme is split into two groups of species. The set of differential equations of one part, which involves the most important species and reactions in methane-air flames, is solved first; the remaining species are solved in a post-processing step. A further reduction in computational effort is achieved by adopting steady-state assumptions for intermediates. The computational effort for the first stage is much smaller than for a complex computation with the full mechanism because the number of major species is relatively small (16 instead of 51). As the species are solved simultaneously in this step, the computational effort depends quadratically on the number of species [8, 9]. The computational effort for the post-processing step is also relatively small due to the fact that the major species, flow, and temperature fields are fixed. Therefore, the set of equations is less stiff. The Miller and Bowman reaction mechanism, updated with the more recent reaction rate data of Glarborg et al. [3], is used and is referred to as the modified Miller and Bowman reaction mechanism. Furthermore, we also used the mechanism of Glarborg et al., which is a subset of the latter, while for the computation of the major combustion species the skeletal mechanism [5] was employed. In the post-processing code, this reaction mechanism is compared with the reaction scheme that includes the nitrogen chemistry. All species (except *NO* and *HCN*) that are part of the complementary part of the two reaction mechanisms are indicated as steady-state species. Differential equations are solved for *NO* and *HCN*. These are given by

$$\rho \mathbf{v} \nabla Y_i - \nabla(\rho D_i \nabla Y_i) = \dot{\rho}_i, \tag{1}$$

where Y_i denotes the mass fraction of species i, ρ the density, v the flow velocity, D_i the diffusion coefficient for species i, and $\dot{\rho}_i$ the chemical source term. In addition, the diffusion coefficients of *NO* and *HCN* are assumed to be equal, and for both species a unit Lewis number ($\mathrm{Le}_i = \lambda/(\rho D_i c_p) = 1$) is applied. Computations with other values for the diffusion coefficients indicate that the sensitivity of the results to the Lewis number is extremely small (less than 0.5% if the diffusion coefficient is varied by a factor of 2).

For the remaining species (not in the initial reaction scheme), steady-state assumptions are applied, given by

$$\dot{\rho}_i = M_i \sum_{j=1}^{N_r} \nu_{ij} r_j = 0, \tag{2}$$

where ν_{ij} are the stoichiometric coefficients, r_j the reaction rate of reaction, j and N_r the number of reactions.

The chemical source term of a steady-state species i is split into "production" and "destruction" parts: $\dot{\rho}_i = \dot{\rho}_i^{(+)} - \dot{\rho}_i^{(-)}$. As the reaction rate of the jth reaction depends on the concentrations of the reacting species, the destruction part of the source term of this reaction, $r_j^{(-)}$, depends explicitly on the concentration c_i of species i and may be written as $r_j^{(-)} = c_i * \gamma_{ij}$, where γ_j is given by

$$\gamma_{ij} = k_j^{(-)} (c_i)^{\nu_{ij}^{(-)}-1} \prod_{m=1,\, m\neq i}^{N} (c_m)^{\nu_{mj}^{(-)}}, \tag{3}$$

where c_i denotes the concentration of species i, and $k_j^{(-)}$ denotes the reaction rate of reactions in which steady-state species i reacts with other species. This reaction rate is equal to the backward reaction rate k_j^b, and $\nu_{ij}^{(-)}$ equals ν_{ij} if the jth reaction produces species i, thus if ν_{ij} is positive. Otherwise, $k_j^{(-)}$ is equal to the forward reaction rate k_j^f, and $\nu_{ij}^{(-)}$ equals $-\nu_{ij}$.

Note that most reactions are two-body reactions, so that $\nu_{ij}^{(-)} = 1$. Then, γ_{ij} does not depend on the concentration of the steady-state species i. The decoupling into reactions that form or remove a steady-state species makes it possible to formulate an explicit expressing for the steady-state species from Eq. 2:

$$c_i = \frac{\sum_{j=1}^{N_r} \nu_{ij} r_j^{(+)}}{\sum_{j=1}^{N_r} \nu_{ij} \gamma_{ij}}. \tag{4}$$

The number of steady-state equations equals $(N - N_s - 2)$, where N is the total number of species in the reaction scheme, and N_s is the number of major species.[1]

[1] Here, $N_s = 16$, the number of species in the skeletal mechanism.

3. DISCRETIZATION AND SOLUTION METHOD

The differential equations (1) are discretized using the finite-volume technique as presented by Thiart [6]. Also, a modification of this discretization is used here in which the source terms are not weighted (with the function $W(P) = 1/P - 1/(e^P - 1)$ depending on the local peclet number P [6]). The effect of the difference in discretization used for the source term is considered. For the two-dimensional flame, the source term is not weighted. The discretization coefficients depend on temperature, density, diffusion coefficients, flow velocity, and grid-spacing only, which do not change during the post-processing step. Therefore, the discretization coefficients may be considered constant, so that they have to be computed only once. The grid used for the two-dimensional flame computations is locally refined during the first computational step. A static refinement procedure is used [7, 8]. An example of a refined grid is shown in Fig. 4.

The steady-state equations and the differential equations, treated in the post-processing step, are coupled. Due to the reduced stiffness, the differential equations are solved sequentially using a tridiagonal matrix equation solver, in contrast to complex computations using the full mechanism where all equations are solved simultaneously using Newton's method [8, 9]. The discretized differential equations for the two-dimensional flame are solved by the ADI method. Before the equations for *NO* and *HCN* are solved, the steady-state species are solved in an inner iteration loop, in which the chemical source terms of *NO* and *HCN* are also computed. This inner iteration procedure solves Eq. 4 sequentially for all steady-state species until the relative variations in the source terms of *NO* and *HCN* in successive iterations is small enough (e.g., $< 10^{-8}$). To achieve convergence, the solution is damped. Typical values for the damping coefficient are 0.1 for *NO* and *HCN*, and 0.8 for the steady-state species.

4. ONE-DIMENSIONAL FLAMES

Results of the post-processing method applied to one-dimensional flames are presented. First, the differences between the discretization methods are considered. Then, results of the post-processor using different reaction mechanisms are compared with complex computations and measurements.

The effect of the differences in the source term discretization is considered by using different grids (see Fig. 1). One grid is coarse at the end of the domain, the second grid has more points at the end of the domain, while the total number of grid points is equal (100). The relative difference in the mass fractions of the major species (of the skeletal mechanism) found with the two grids is less than a few percent. Furthermore, increasing the number of grid points did not have a significant influence on the solution.

The *NO* profiles, obtained in the post-processing step (using the reaction scheme of Glarborg), however, deviate by up to 15%. There are also considerable deviations between computations using the discretization methods for the grid that is coarse at the end of the domain. The differences between the discretization methods are much smaller for

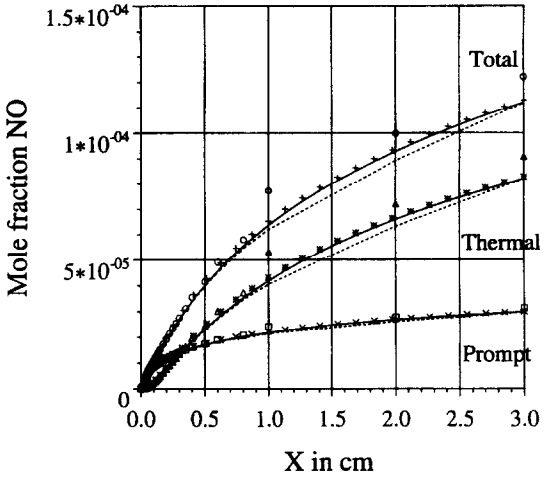

Fig. 1. Profiles of *NO* mole fractions on different grids with different source term discretizations. Lines denote computations with weighted source term; continuous lines correspond to a grid that is fine in the post-flame zone; and dashed lines to a grid that is coarse in the post-flame zone. Position of the markers corresponds to the position of grid points. The ∘, △, and □ markers correspond to the dashed lines, using the nonweighted sources term. The +, *, and × markers correspond to the continuous lines. Mass flow rate is 0.0395 g/cm^{2}s, and the equivalence ratio Φ is 1.0.

the grid, that has less points in the post-flame zone. These results indicate that special attention has to be paid to the grid for accurate *NO* predictions. This means that a (non-equidistant) grid suitable to predict the major species may be too coarse for accurate prediction of *NO* in the post-processing step.

To test the errors introduced by the approximations in the post-processing method, we compared results of the post-processing method with complex computations with the full mechanism. For the post-processor, we used the reaction scheme of Glarborg et al. [3] and the modified Miller and Bowman scheme [2]. For the complex computations (solving differential equations for all 51 species), we used the latter only. To eliminate effects caused by differences in flame temperature of burner-stabilized flames due to differences in adiabatic burning velocity[2] found with the skeletal mechanism and the (modified) scheme of Miller and Bowman, adiabatic flames are considered.

Furthermore, to prevent differences in the chemical equilibrium composition found with the various mechanisms, all reactions are assumed to be reversible, and reverse reaction rates are obtained from the equilibrium constants.

The results of the post-processing method and the complex computations are presented in Fig. 2. The differences are small. This confirms the assumption that decoupling of the major species and the application of steady-state assumptions have a negligible influence on the results. Furthermore, the differences between the results of post-calculations with the modified Miller and Bowman mechanism and the Glarborg et al. mechanism are also small. This means that the species and reactions omitted in the reduced mechanism of the latter are of minor interest. It should, however, be stressed that the assumptions of all reactions being reversible, and that all reverse reaction rates are obtained by use of the equilibrium constants, are of major importance. It appeared that these modifications may result

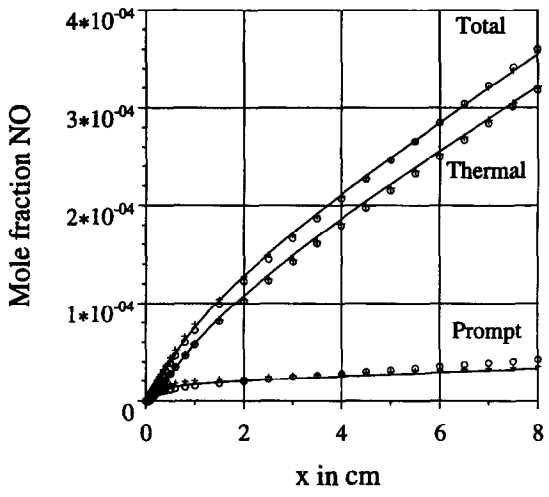

Fig. 2. Results of post-processing method (markers) and complex computations (lines) for an adiabatic stoichiometric methane-air flame: (∘), skeletal mechanism for major species and modified Miller and Bowman scheme for post-processing step; (+), skeletal scheme for major species and Glarborg scheme for post-processing step. Complex computations performed with modified Miller and Bowman scheme.

in differences of up to 10% in the final *NO* mole fractions. The computational effort of the post-processing method (using the Glarborg et al. mechanism) is roughly a factor of 20 lower than the computational effort for the complex computations solving all differential equations for the species simultaneously using the full reaction mechanism. If the modified reaction mechanism of Miller and Bowman is used in the post-processing step, the computational effort is roughly twice as large as with the Glarborg et al. mechanism.

To validate the post-processing method and the reaction mechanisms, the results are compared with measurements of *NO* above a ceramic foam surface burner. The measurements are performed using a cooled suction probe, and the gas samples are analyzed by chemoluminiscence. The code has been extended to model flames on this burner. The ceramic burner and the measurements are described in more detail in Bouma et al. [10]. To model flames on this burner, again the skeletal mechanism is used to predict major species concentrations, and the scheme of Glarborg et al. [3] is used for the post-processing step. Some results are shown in Fig. 3, which agree well with

[2] The adiabatic burning velocities found with the Miller and Bowman and skeletal schemes are 41.4 cm/s and 44.8 cm/s, respectively.

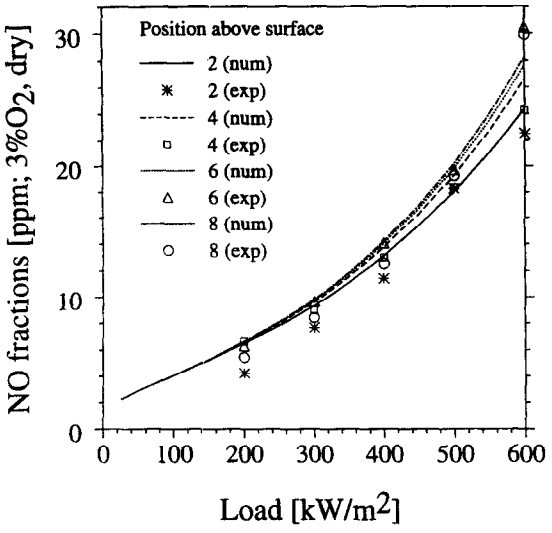

Fig. 3. Comparison of measurements and computations of *NO*, formed in methane-air flames (Φ = 0.77) stabilized on radiant ceramic foam burner.

the measurements. The differences are smaller than 20%. This is within the accuracy range of the measurements. The accuracy of the computations is of the same order of magnitude, due to uncertainties in the reaction rate data.

5. TWO-DIMENSIONAL FLAMES

A single-shot burner in a confined environment with cooled walls now is considered. The burner geometry and the locally refined mesh used for the computations are shown in Fig. 4. The computational domain is 8 mm high and 6 mm wide. In the computations only one half slot (2 mm wide) is modeled with symmetrical boundary conditions at the center line. The burner edge is 1 mm high and 0.9 mm wide. The complex computation of the major combustion species is described in more detail by Somers and de Goey [11]. Post-processing is performed using the reaction scheme of Glarborg et al. [3]. The chemical source terms of the thermal and total *NO* formation are presented in Figs. 5 and 6, respectively. Contour lines of the temperature are also presented in these figures.

It can be seen that the *NO* source term reaches its maximum between 1700 *K* and 1800 *K*. This maximum is caused by the prompt *NO* mechanism. The thermal source term reaches its maximum at a higher temperature.

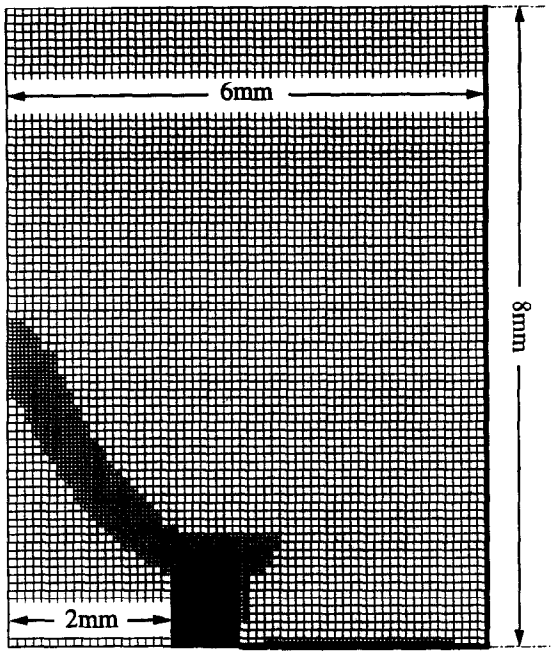

Fig. 4. Computational domain and locally refined mesh for single-slot burner. Thick lines indicate walls.

This can be seen more clearly in Fig. 7, where the source terms on the center line (x = 0) are presented. The prompt *NO* production rate reaches its maximum on the center line in the flame-front at y = 4.2 mm, whereas the largest thermal *NO* production rate is located at y = 5.5 mm, in the post-flame zone. Moreover, it

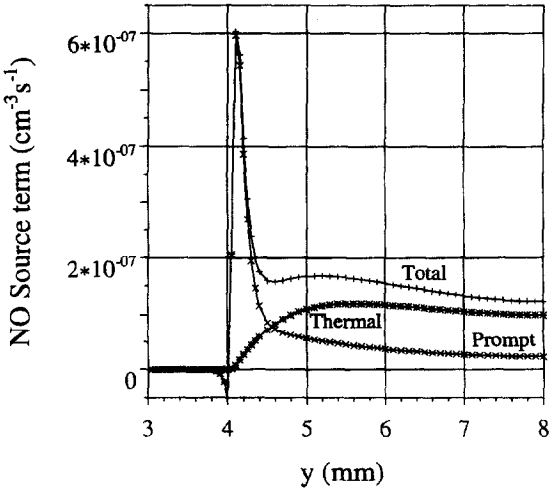

Fig. 7. Source terms of thermal, prompt, and total *NO* formation on center line for slot burner.

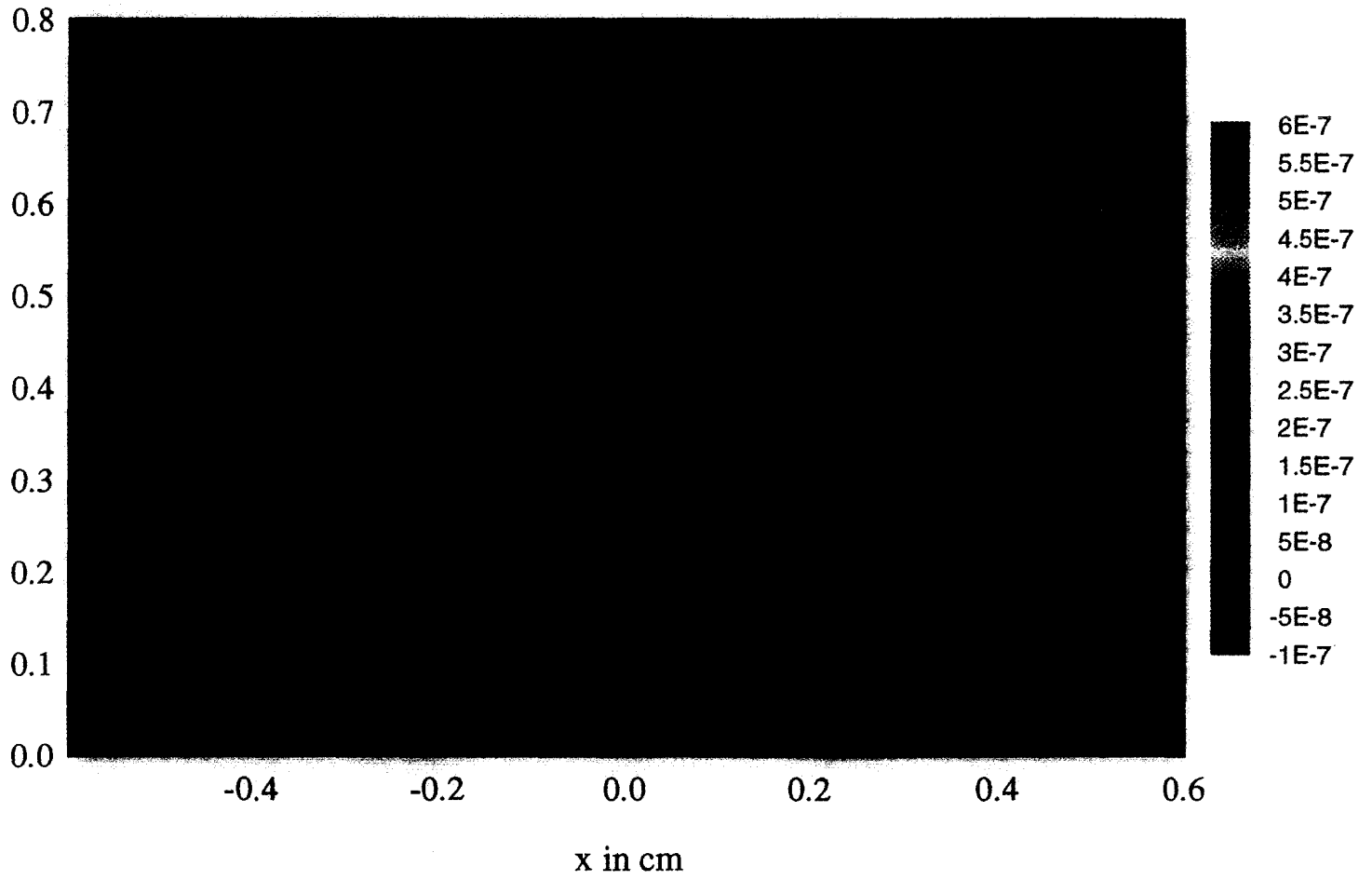

Fig. 5. False color plot of the prompt *NO* source term (in $cm^{-3}\ s^{-1}$) and temperature contour lines for the single-slot burner.

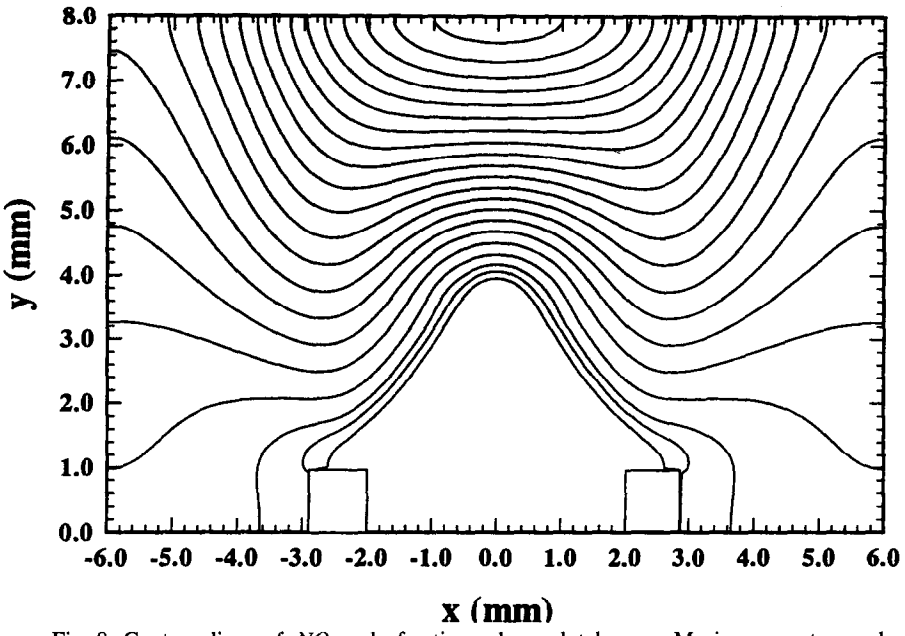

Fig. 8. Contour lines of *NO* mole fractions above slot burner. Maximum contour value is 58 ppm.

can be observed that the prompt *NO* source term is also quite large in the post-flame area. Contour lines of *NO* mole fraction are shown in Fig. 8. Maximum *NO* concentrations are observed on the center line above the flame. Although the maximum value of the prompt *NO* source term is much larger than the maximum thermal source term, most *NO* (about 60%) is formed by the thermal mechanism on the center line at the end of the domain.

Considering the results of the one- and two-dimensional computations and the measurements, we may conclude that the prompt *NO* mechanisms may have a significant contribution to total *NO* formation. The ratio of thermal and prompt *NO*, however, strongly depends on the temperature of the flame and the position above the burner. Most of the *NO* formed in the adiabatic flames is formed by the thermal *NO* mechanism. The flames stabilized on burners show a significant contribution of the prompt mechanism.

6. CONCLUSIONS

One- and two-dimensional flame computations have been performed, including detailed nitrogen chemistry. The major combustion species and radicals are computed with a simplified reaction scheme, without nitrogen chemistry. The remaining nitrogen compounds and species of the C_2-chain are calculated in a post-processing step. Results of one-dimensional *NO* computations for a porous ceramic foam burner agree to within 20% of measured values. The differences between measured and computed values are of the same order of magnitude as the inaccuracy in the reaction rate data and experiment. It is observed that, for modeling *NO* formation, the grid spacing in the post-flame zone needs special attention. A grid that is fine enough to predict major species may be too coarse to predict accurate *NO* formation. Furthermore, differences between computations of one-dimensional adiabatic flames using several reaction schemes are small. The same is true of the differences between the results from application of the post-processor method and detailed computations. The inaccuracies introduced by decoupling the major combustion species and other species are much smaller than the inaccuracies resulting from errors in the reaction rate data. The computational effort in applying the post-

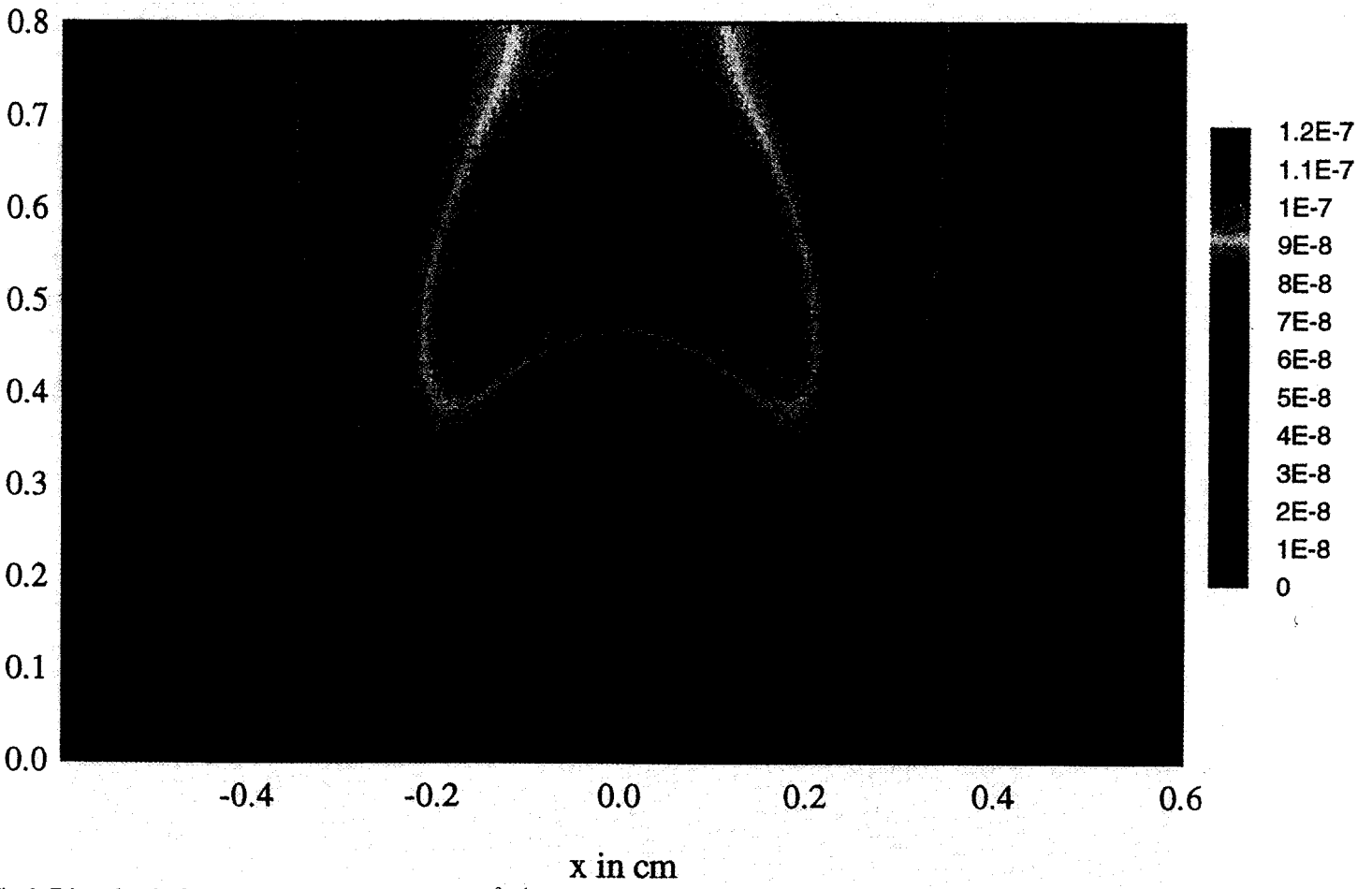

Fig. 6. False color plot for the thermal *NO* source term (in $cm^{-3}\ s^{-1}$) and temperature contour lines for the single-slot burner.

processing method, however, is only a few percent of the computational effort necessary to solve the complex system in one step.

The application of the post-processor method for two-dimensional flames makes it possible to study the formation of *NO* by the thermal as well as the prompt mechanism, while the computational effort is not much larger than the computation effort for the first computational step using a simple reaction mechanism, including only major species.

The support of Gastec N.V. and NOVEM, the Netherlands, is gratefully acknowledged. The authors thank Bart Somers for the results of the two-dimensional complex flame computations and Peter Bouma for the results of the measurements.

REFERENCES

1. Bowman, C. T., *Twenty-Fourth Symposium (International) on Combustion*, The Combustion Institute, Pittsburgh, 1992, p. 859.
2. Miller, J. A., and Bowman, C. T., *Prog. Ener. Combust. Sci.* 15:287 (1989).
3. Glarborg, P., Lilleheie, N. L., Byggstøyl, S., Magnussen, B. F., Kilpinen, P., and Hupa, M., *Twenty-Fourth Symposium (International) on Combustion*, The Combustion Institute, Pittsburgh, 1992, p. 889.
4. Eggels, R. L. G. M., Somers, L. M. T., de Goey, L. P. H., and Nieuwenhuizen, J. K., *Proc. Second International Conference on Combustion for a Clear Environment*, Lissabon, 1993, p. 12.2.
5. Smooke, M. D., *Lecture Notes in Physics*, Springer-Verlag, Berlin, New York, 1991, p. 1.
6. Thiart, G. D., *Numerical Heat Transfer Part B*, Vol. 17, 1990, p. 43.
7. Lange, H. C., Ph.D. thesis, Eindhoven University of Technology, the Netherlands, 1992.
8. Somers, L. M. T., Ph.D. thesis, Eindhoven University of Technology, the Netherlands, 1994.
9. Kee, R. J., Grcar, J. F., Smooke, M. D., and Miller, J. A., Sandia Report SAND85-8240, Sandia National Laboratories, Livermore, CA, 1985.
10. Bouma, P. H., de Goey, L. P. H., Nieuwenhuizen, J. K., and van der Drift, A., *Proc. Second International Conference on Combustion for a Clear Environment*, Lissabon, 1993, p. 36.
11. Somers, L. M. T., and de Goey, L. P. H., *Combust. Sci. Technol.* 108:121 (1995).

Received 17 March 1995; revised 15 September 1995